Observation of magnetic vortex pairs at room temperature in a planar α-Fe_2O_3/Co heterostructure.

F. P. Chmiel[1], N. Waterfield Price[1], R. D. Johnson[1], A. Lamirand[2], J. Schad[3], G. van der Laan[2], D. T. Harris[3], J. Irwin[4], M. S. Rzchowski[4], C.-B. Eom[3] & P. G. Radaelli[1*]

[1] *Clarendon Laboratory, Department of Physics, University of Oxford, Parks Road, Oxford OX1 3PU, United Kingdom*

[2] *Diamond Light Source, Harwell Science and Innovation Campus, Didcot OX11 0DE, United Kingdom*

[3] *Department of Materials Science and Engineering, University of Wisconsin-Madison, Madison, Wisconsin 53706, USA*

[4] *Department of Physics, University of Wisconsin-Madison, Madison, Wisconsin 53706, USA*

Vortices are among the simplest topological structures, and occur whenever a flow field 'whirls' around a one-dimensional core. They are ubiquitous to many branches of physics, from fluid dynamics to superconductivity and superfluidity,[1] and are even predicted by some unified theories of particle interactions, where they might explain some of the largest-scale structures seen in today's Universe.[2] In the crystalline state, vortex formation is rare, since it is generally hampered by long-range interactions: in ferroic materials (ferromagnetic and ferroelectric), vortices are only observed when the effects of the dipole-dipole interaction is modified by confinement at the nanoscale,[3–5] or when the parameter associated with the vorticity does not couple directly with strain.[6] Here, we present the discovery of a novel form

of vortices in *antiferromagnetic* (AFM) hematite (α-Fe_2O_3) epitaxial films, in which the primary whirling parameter is the staggered magnetisation. Remarkably, ferromagnetic (FM) topological objects with the same vorticity and winding number of the α-Fe_2O_3 vortices are imprinted onto an ultra-thin Co ferromagnetic over-layer by interfacial exchange. Our data suggest that the ferromagnetic vortices may be *merons* (half-skyrmions, carrying an out-of-plane core magnetisation), and indicate that the vortex/meron pairs can be manipulated by the application of an in-plane magnetic field, $H_{\|}$, giving rise to large-scale vortex-antivortex annihilation.

α-Fe_2O_3 is a 'classic' room-temperature antiferromagnet, with a Neèl temperature of 948 K and the trigonal corundum crystal structure (space group $R\bar{3}c$). The Fe moments lie in the basal ab plane and are antiferromagnetically ordered along c (Fig. 1). We grew 10 nm-thick α-Fe_2O_3 epitaxial films with a Co (1 nm) / Al (1 nm) overlayer on a (0001)-Al_2O_3 substrate by magnetron sputtering (see Methods). The Co layer was confirmed to be ferromagnetically ordered, with easy-plane anisotropy, by Magneto-Optical Kerr Effect magnetometry (MOKE, see supplementary information) and its coercive field was found to be ~ 8 mT. Vector-mapped x-ray magnetic linear (for α-Fe_2O_3) and circular (for Co) dichroism photoemission electron microscopy (XMLD-PEEM and XMCD-PEEM) images were collected at room temperature and zero applied magnetic field at the Fe-L_3 and Co- L_3 edges respectively, using the I06 beamline at the Diamond Light Source, Didcot, UK. Exploiting the anisotropy of the XMLD / XMCD signal, data collected at different sample rotations were combined, to determine absolutely the direction parallel/anti-parallel to the AFM spins (hereafter referred to as the AFM axis) and the Co spin direction at the same positions on the surface of the sample (Fig. 1).[7–10] We found that the α-Fe_2O_3 spins are perpendicular to both the crystallographic c-axis and to one of the three 2-fold axes (magnetic space group $C2/c$), as previously reported.[11,12] The three possible orientations of the AFM moments, related by the broken 3-fold rotation axis of the crystallographic structure, form an intricate domain structure (Fig. 2 a) at the scale of a few tens of nm. One prominent feature of these images is the presence of 'pinch-points' between α-Fe_2O_3 domains of the same orientation. Around these points, domains are typically arranged in a 6-sector pinwheel, colors alternating as either R-G-B-R-G-B or R-B-G-R-B-G clockwise around their common core (here, 'R' represents α-Fe_2O_3 domains with the AFM spin direction parallel to [2,1,0], 'B' to [1,2,0] and 'G' to [-2,1,0] in the hexagonal setting of the unit cell, see Fig. 1 c). Overall, the domain morphology is strikingly reminiscent both of the disclination domains in liquid crystals[13] and of the cloverleaf *ferroelectric* domain patterns imaged in the hexagonal manganite $YMnO_3$ by piezoelectric force microscopy (PFM), pointing towards a common phenomenology in completely different contexts.[6,14] Remarkably, at the phenomenological level there is an almost complete analogy between AFM ordering in α-Fe_2O_3 and structural ordering in $YMnO_3$, so that the terms in the Landau free energy expansion that contain only the principal order parameter are exactly the same up to at least the sixth order.[15] There are, however, also some important differences: in the case of α-Fe_2O_3, the order parameter is magnetic rather than structural and couples linearly to a weak ferromagnetic moment. Secondly, ordering in α-Fe_2O_3 breaks 3-fold symmetry, so that the order parameter is associated with a physical orientation in space (i.e., the orientation of the AFM spins). On this basis and following the $YMnO_3$ analogy, the Fe L_3 XMLD-PEEM images can be straightforwardly interpreted: the 'pinch-points' are the *loci* of anti-phase boundaries, where the AFM order parameter has the same orientation but changes sign across the pinched boundary. Such boundaries are unfavourable energetically and are reduced to points (lines parallel to the film normal in 3 dimensions) during the domain formation, whilst the most favourable 60° domain walls end up dominating. We conclude that the 'pinwheels' we observe are AFM vortices (R-G*-B-R*-G-B*; winding number +1) and anti-vortices (R-B*-G-R*-B-G*; winding number -1), asterisks denoting time inversion. The vortices /anti-vortices form a relatively dense network, with approximately 40 instances over a 80 μm^2 area. There are several closely-bound vortex/antivortex pairs, as well as isolated vortices, suggesting that the sample has been quenched without undergoing a Kosterlitz-Thouless transition.[16] Thus far, AFM vortices had only been created in nanoscale disk heterostructures by imprinting from FM vortices,[17,18] and have never been previously observed in a homogeneous system.

Co- L_3 XMCD-PEEM images (Fig. 2 b) reveal the Co FM domain morphology over the same region of the sample and strongly suggest an imprinting of the α-Fe_2O_3 features on the FM Co over-layer which, on a non-magnetic substrate, would typically be uniformly magnetised over this length-scale. The Co spins tend to align strongly *parallel* to the α-Fe_2O_3 spin direction, so that the α-Fe_2O_3 and the Co vector maps share a similar morphology (Fig. 2 a and b). In addition to the domain geometry, the topological features of the α-Fe_2O_3 magnetism are also imprinted on the Co over-layer. In particular, FM vortices and anti-vortices are clearly visible on top of corresponding α-Fe_2O_3 features with the *same* winding number (Fig. 2 a and b) with the vortex cores being precisely aligned within the resolution of our measurements. Figure 3 displays numerical differentiation of the XMCD-PEEM images, which enabled us to pinpoint exactly the location and nature of the FM vortices and antivortices: clock-wise and anticlock-wise vortices are most apparent in the maps of the curl of the Co magnetisation, while antivortices display an angular alternation of curl in different sectors. The typical vortex core size, extracted, from the full width at half maximum of maps of the magnitude of the Co magnetisation (Fig. 3 c) is of the order of 100 nm and appears to be limited by the resolution of our experiment. Once again, we emphasise that FM vortices were only previously observed in nanodots.[5,19]

In magnetic vortex structures, even with strong planar-anisotropy, the magnetisation often points out-of-the plane at the vortex core to satisfy unfavourable exchange and dipole interactions.[20] Indeed, in our XMCD-PEEM images we observe a reduction of the magnitude of the XMCD, sensitive only to the in-plane magnetisation (Fig. 3 c), which is compatible with the presence of an out-of-plane component of the Co spins at the vortex core. This raises the intriguing possibility that the FM topological structures we observe are *merons/antimerons* (also known as half-skyrmions)[21] rather than planar vortices/antivortices (Fig. 3 a), imprinted by interfacial exchange with the adjacent AFM vortex/anti-vortex in the α-Fe_2O_3 film. Although the out-of-plane magnetic moment of the meron core is not a topological invariant, reversing it by a global rotation in spin space requires 'unwinding' the meron, which is strongly disfavoured by the easy-plane anisotropy, meaning the moment at the core should be stable to small external perturbation.

We found it is possible to manipulate the vortex/meron pairs by the application of moderate magnetic fields. To achieve this, we removed the sample from the PEEM chamber, applied a 100 mT field parallel to $[1,1,0]_{\mathrm{h}}$ and re-aligned the sample in the same position under the electron microscope. Figures 2 and 4 show the remarkable end result of this process: domains not involved in 'pinch-points' are largely invariant, (e.g., Fig. 4 c and d), meaning that the large-scale features of the vector map are mostly unchanged. However, large scale vortex/antivortex annihilation has clearly occurred, removing all 'pinch-points' from the α-Fe_2O_3 film, Fig. 4 a and b. This phenomenon is confirmed by the Co L_3 XMCD-PEEM vector map (Fig. 2 d) of the Co over-layer: although the Co spins maintain a strong tendency to align along the direction of the α-Fe_2O_3 staggered magnetisation, the vast majority of FM vortex/merons have disappeared.

Our observation of a dense population of coupled AFM/FM vortex pairs in a planar homogeneous α-Fe_2O_3/Co heterostructure indicates multiple avenues for exploitation in both fundamental and applied research. At the fundamental level, this system represents the first purely magnetic realisation of the Kibble-Zurek model with discrete Z_6 symmetry, which has been previously studied in as a structural realisation in $YMnO_3$.[22] The close proximity to room temperature of the first-order Morin transition ($\sim$ 260 K for bulk α-Fe_2O_3, tuneable by film thickness and doping),[23] below which the Fe spins flop along the c axis and all AFM vortices must disappear, provide a further opportunity to study the first-order analogue of the Kibble-Zurek model, in which the string density is controlled by nucleation rather than fluctuations. On the applied side, FM merons can be thought as topologically protected spin 'bits', and could be very appealing for information storage in both pinned and free forms. A regular array of pinned merons, arranged for example in a cross-point architecture,[24] could store information in the magnetisaton of the FM meron core, in analogy to proposed memories based on arrays of FM nanodots.[25] If a population imbalance between merons and antimerons could be created, free merons could be produced by cooling below the Morin transition. Such a hypothetical device could serve as a source for 'meron racetrack memories', similar to those currently considered for skyrmions.[26,27]

Acknowledgements

We acknowledge Diamond Light Source for time on Beam Line I06 under Proposal SI16338 and SI15088. We thank S. Parameswaran for discussions and T. Hesjedal and S. Zhang for assistance with initial film growth. The work done at the University of Oxford (F. P. C, N. W. P., R. D. J., and P. G. R.) is funded by EPSRC Grant No. EP/M020517/1, entitled Oxford Quantum Materials Platform Grant. The work at University of Wisconsin-Madison (J.S., J. I., M. S. R. and C.-B. E.) supported by the Army Research Office through Grant No. W911NF-13-1-0486 and W911NF-17-1-0462. R. D. J. acknowledges support from a Royal Society University Research Fellowship.

Author Contributions

F. P. C., N. W. P., R. D. J. and A. L. performed the experiment. F. P. C. and A. L. performed the data reduction. F. P. C and N. W. P. performed the data analysis. J. S grew the films. D. T. H. made the α-Fe_2O_3 sputtering target. J. S and F. P. C. characterised the epitaxial relation of the films. J. I. performed the MOKE measurement. G. v. L. performed calculations of the XMLD signal. P. G. R conceived and designed the experiment and supervised the analysis together with R. D. J, while C.-B. E. supervised the film growth. M. S. R. supervised the MOKE measurement. P. G. R. and F. P. C wrote the first draft of the manuscript. All authors discussed and contributed to the manuscript.

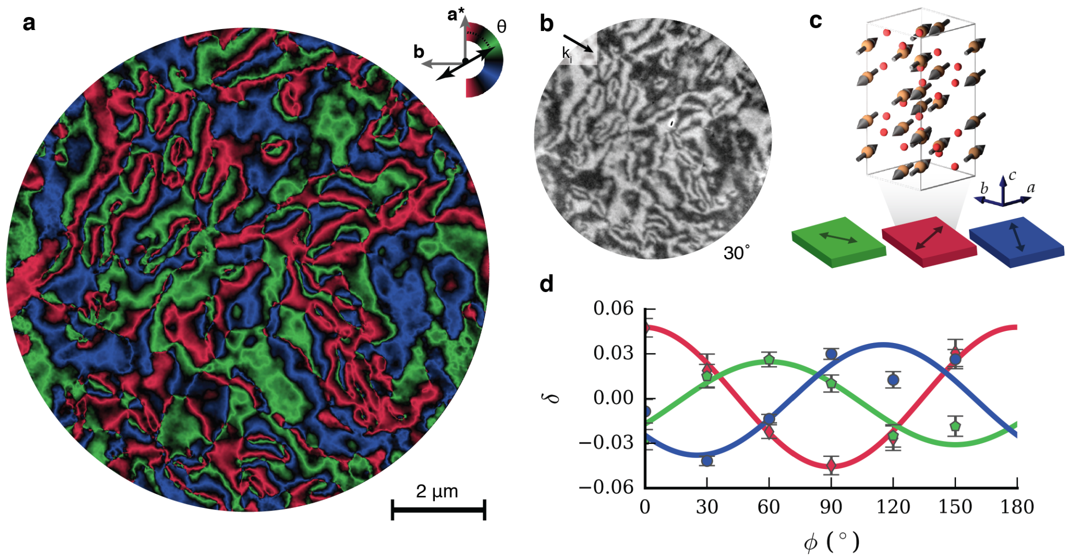

Figure 1: Vector map of α-Fe_2O_3 antiferromagnetic domain configuration from x-ray photoemission microscopy. a, α-Fe_2O_3 domain structure constructed using the anisotropy of the XMLD signal. **b,** Measured XMLD signal for a single incident x-ray direction (azimuth), denoted by the solid black arrow. **c,** Graphic displaying the magnetic unit cell of α-Fe_2O_3 and the three orientational antiferromagnetic domains. **d,** Mean dichorism (XMLD signal), as a function of azimuth, for three 15 x 15 pixel regions, one in each of the three identified domains. Solid lines are the fits assuming a single AFM axis in each region.

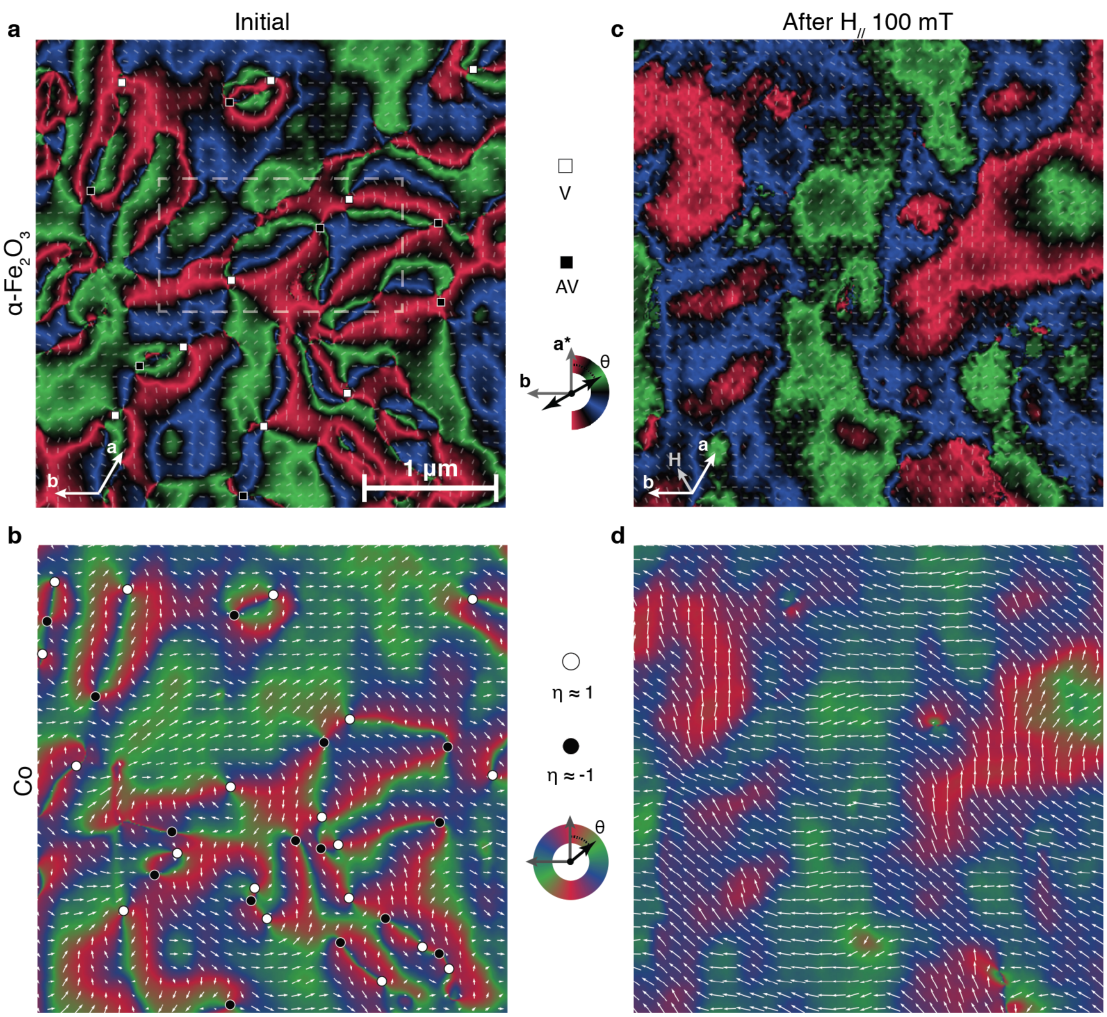
a
Initial
c
After H// 100 mT
α-Fe2O3
V
AV
a*
θ
b
a
1 μm
H
Co
η ≈ 1
η ≈ -1
d

Figure 2 ***(previous page)*****: Magnetic domain structure of α-Fe_2O_3 / Co film. a,** Initial α-Fe_2O_3 antiferromagnetic domain structure as determined by vector - mapped XMLD-PEEM. White (black) squares indicate the approximate centre of identified vortex (anti-vortex) cores. White bars display the measured antiferromagnetic axis for a ten square pixel region; color represents the angle of the antiferromagnetic axis for each pixel measured clockwise from a^*. The dashed white box shows the region of interest used in Fig. 3.**b,** Co spin vector map determined from XMCD-PEEM, white (black) circles are topological defects with a winding number of 1 (-1), see Methods for details. White arrows show the local in-plane spin orientation of the Co film for a ten square pixel region and color the angle of the spin, for each pixel, measured clockwise from a^*. **c-d,** α-Fe_2O_3 and Co vector map after application of an *ex-situ*, 100 mT magnetic field along $[1,1,0]_\mathrm{h}$. All images were recorded at the same position on the sample surface.

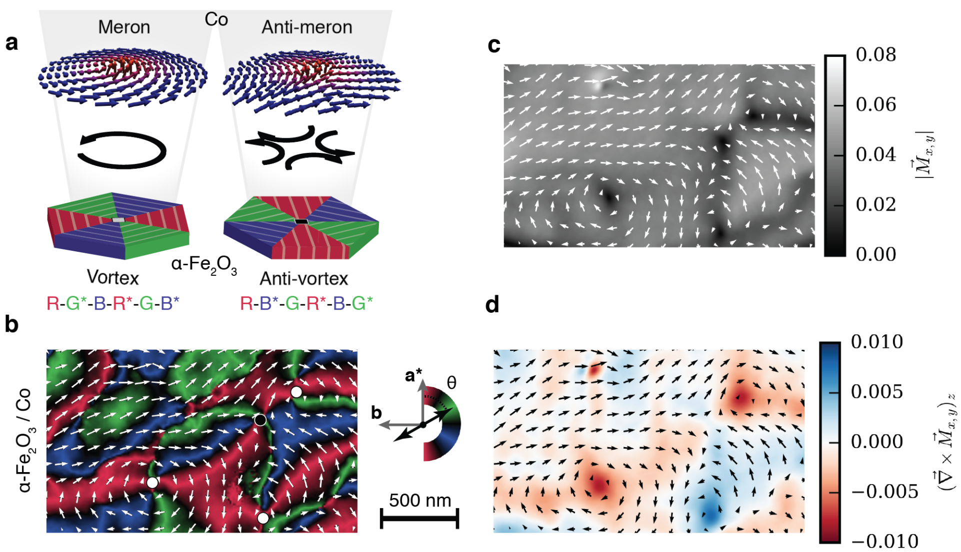

Figure 3: Topological defects in α-Fe$_2$O$_3$ and Co. a, Graphic demonstrating coupling between α-Fe$_2$O$_3$ (anti-)vortices and Co (anti-)merons. **b,** Combined ferromagnetic (white arrows) and antiferromagnetic (colour) α-Fe$_2$O$_3$ / Co film domain structure for a small area of our film, shown by the dashed box in Fig. 2a. White (black) circles show topological defects with a winding number of +1(-1). **c** Measured magnitude of Co magnetisation in the sample plane. The intensity reduction at the vortex cores is compatible with the meron picture (see text), although resolution smearing could produce similar effects. **d,** $\hat{z}$ component of the curl of the Co vector map.

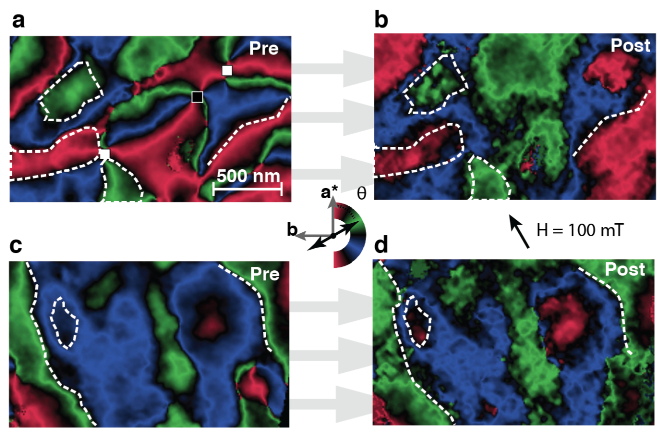

Figure 4: Vortex annihilation with *ex-situ* applied field. a-d, Measured α-Fe_2O_3 domain configuration in two different regions of the sample before, a and c, and after, b and d, application of the 100 mT in-plane ($[1,1,0]_h$) magnetic field. The Co spins share a similar evolution see Fig. 2 b and d.

1. Zurek, W. H. Cosmological experiments in superfluid helium? *Nature* **317**, 505–508 (1985).

2. Kibble, T. W. B. Topology of cosmic domains and strings. *J. Phys. A: Math. Gen.* **9**, 1387–1398 (1976).

3. Zheng, Y. & Chen, W. Characteristics and controllability of vortices in ferromagnetics, ferroelectrics and multiferroics. *Rep. Prog. Phys.* **80**, 086501 (2017).

4. Yadav, A. K. *et al.* Observation of polar vortices in oxide superlattices. *Nature* **530**, 198–201 (2016).

5. Cowburn, R. P., Koltsov, D. K., Adeyeye, A. O., Welland, M. E. & Tricker, D. M. Single-domain circular nanomagnets. *Phys. Rev. Lett.* **83**, 1042 (1999).

6. Choi, T. *et al.* Insulating interlocked ferroelectric and structural antiphase domain walls in multiferroic $YMnO_3$. *Nat. Mater.* **9**, 253 (2010).

7. Hallsteinsen, I. *et al.* Magnetic domain configuration of (111)-oriented $LaFeO_3$ epitaxial thin films. *Appl. Phys. Lett. Mater.* **5**, 086107 (2017).

8. Waterfield Price, N. *et al.* Coherent magnetoelastic domains in multiferroic $BiFeO_3$ films. *Phys. Rev. Lett.* **117**, 177601 (2016).

9. Alders, D. *et al.* Magnetic x-ray dichroism study of the nearest-neighbor spin-spin correlation function and long-range magnetic order parameter in antiferromagnetic NiO. *Europhys. Lett.* **32**, 259 (1995).

10. Scholl, A., Ohldag, H., Nolting, F., Stöhr, J. & Padmore, H. A. X-ray photoemission electron microscopy, a tool for the investigation of complex magnetic structures. *Rev. Sci. Instrum.* **73**, 1362–1366 (2002).

11. Chen, P., Lee, N., McGill, S., Cheong, S.-W. & Musfeldt, J. Magnetic-field-induced color change in α-Fe_2O_3 single crystals. *Phys. Rev. B* **85**, 174413 (2012).

12. Marmeggi, J. C., Hohlwein, D. & Bertaut, E. F. Magnetic neutron Laue diffraction study of the domain distribution in α-Fe_2O_3. *Phys. Stat. Sol. (a)* **39**, 57–64 (1977).

13. Nehring, J. & Saupe, A. On the schlieren texture in nematic and smectic liquid crystals. *J. Chem. Soc., Faraday Trans. 2* **68**, 1 (1972).

14. Chae, S. C. *et al.* Direct observation of the proliferation of ferroelectric loop domains and vortex-antivortex pairs. *Phys. Rev. Lett.* **108**, 167603 (2012).

15. Artyukhin, S., Delaney, K. T., Spaldin, N. A. & Mostovoy, M. Landau theory of topological defects in multiferroic hexagonal manganites. *Nat. Mater.* **13**, 42–49 (2013).

16. Kosterlitz, J. M. & Thouless, D. J. Ordering, metastability and phase transitions in two-dimensional systems. *J. Phys. C: Solid State Phys.* **6**, 1181–1203 (1973).

17. Sort, J. *et al.* Imprinting vortices into antiferromagnets. *Phys. Rev. Lett.* **97**, 067201 (2006).

18. Wu, J. *et al.* Direct observation of imprinted antiferromagnetic vortex states in

CoO/Fe/Ag(001) discs. *Nat. Phys.* **7**, 303–306 (2011).

19. Wintz, S. *et al.* Topology and origin of effective spin meron pairs in ferromagnetic multilayer elements. *Phys. Rev. Lett.* **110**, 177201 (2013).

20. Shinjo, T., Okuno, T., Hassdorf, R., Shigeto, K. & Ono, T. Magnetic vortex core observation in circular dots of permalloy. *Science* **289**, 930–932 (2000).

21. Senthil, T., Vishwanath, A., Balents, L., Sachdev, S. & Fisher, M. P. Deconfined quantum critical points. *Science* **303**, 1490–1494 (2004).

22. Griffin, S. M. *et al.* Scaling behavior and beyond equilibrium in the hexagonal manganites. *Phys. Rev. X* **2**, 041022 (2012).

23. Shimomura, N. *et al.* Morin transition temperature in (0001)-oriented α-Fe_2O_3 thin film and effect of Ir doping. *J. Appl. Phys.* **117**, 17C736 (2015).

24. Yu, Y.-S., Jung, H., Lee, K.-S., Fischer, P. & Kim, S.-K. Memory-bit selection and recording by rotating fields in vortex-core cross-point architecture. *Appl. Phys. Lett.* **98**, 052507 (2011).

25. Nakano, K. *et al.* All-electrical operation of magnetic vortex core memory cell. *Appl. Phys. Lett.* **99**, 262505 (2011).

26. Parkin, S. S. P., Hayashi, M. & Thomas, L. Magnetic domain-wall racetrack memory. *Science* **320**, 190–194 (2008).

27. Tomasello, R. *et al.* A strategy for the design of skyrmion racetrack memories. *Sci. Rep.* **4** (2014).